Dr. Arul Vadivel
Department of Pediatrics
Dr. Bernard Thébaud Laboratory

I was born and raised in Tamil Nadu, India. I obtained my PhD degree from one of the CSIR (Council of Scientific and Industrial Research) institutes, the Central Leather Research Institute (CLRI) in Chennai, India. During my PhD program, I developed novel collagen-based biomaterials using GHK peptide for wound healing in normal and diabetic rats and compared them to antimicrobial (pexiganan) peptides and reactive oxygen species-generating enzyme-based materials such as glucose oxidase. My interest in wound healing processes was ideally suited for Dr. Bernard Thébaud's research program at the University of Alberta, where I am currently working on the mechanisms of oxygen-induced lung injury and potential therapeutic strategies. Although oxygen is used to rescue premature babies that have underdeveloped lungs, high concentrations of oxygen for a longer period of time result in a chronic form of lung damage referred to as bronchopulmonary dysplasia (BPD). BPD encompasses arrest of alveolar development with disruption of normal lung alveolarization and vascularization; currently, this disease lacks efficient treatment. My research over the past 5 years with Dr. Thébaud has led to the identification of several novel therapeutic targets for the prevention and treatment of chronic lung diseases, including BPD.

Axonal guidance cues (AGC) are molecules that regulate neural network formation in the nervous system and the outgrowth of axons by acting as attractants or as repellents. AGC are also crucial for angiogenesis and recent studies show that AGC promote organ morphogenesis outside the nervous system. Indeed, AGC are implicated in early lung branching morphogenesis, but their role during alveolarization is unexplored. Based on the above, AGC are appealing candidates in guiding the outgrowth of secondary crests, a mechanism that is crucial for alveolarization.

In this publication we show that: 1) The candidate AGC Ephrin B2 promotes normal alveolarization: *in vivo* airway delivery of Ephrin B2 siRNA arrest alveolar and lung vascular growth; 2) Impaired alveolarization in experimental oxygen-induced BPD is associated with decreased Ephrin B2 signaling; and 3) Activation of EphrinB2 preserves distal lung cells from oxygen toxicity *in vitro* and prevents lung injury and pulmonary hypertension in experimental BPD *in vivo*.

The novel findings of this paper provide proof of concept that the AGC Ephrin B2 promotes normal alveolar growth, preserves alveolar development and prevents pulmonary hypertension in an oxygen-induced model of BPD in newborn rats. Ephrin B2 may have therapeutic potential for preventing alveolar damage and pulmonary hypertension.

I would like to acknowledge all the co-authors on this publication and colleagues in my laboratory. Also I would like to thank Dr. Bernard Thébaud for his mentorship, continuous encouragement, support and his intellectual advice towards my research goal. I am extremely thankful and grateful for his continuous mentorship. As a clinician-scientist, Dr. Thébaud has successfully positioned the research focus of his laboratory at the vital interface that allows the immediate translation of “traditional” biomedical science tools into the clinical environment.

AMERICAN JOURNAL OF

Respiratory and Critical Care Medicine®

ATS
We help the world breathe
PULMONARY • CRITICAL CARE • SLEEP

VOLUME 185
NUMBER 5
MARCH 1 2012
www.thoracic.org

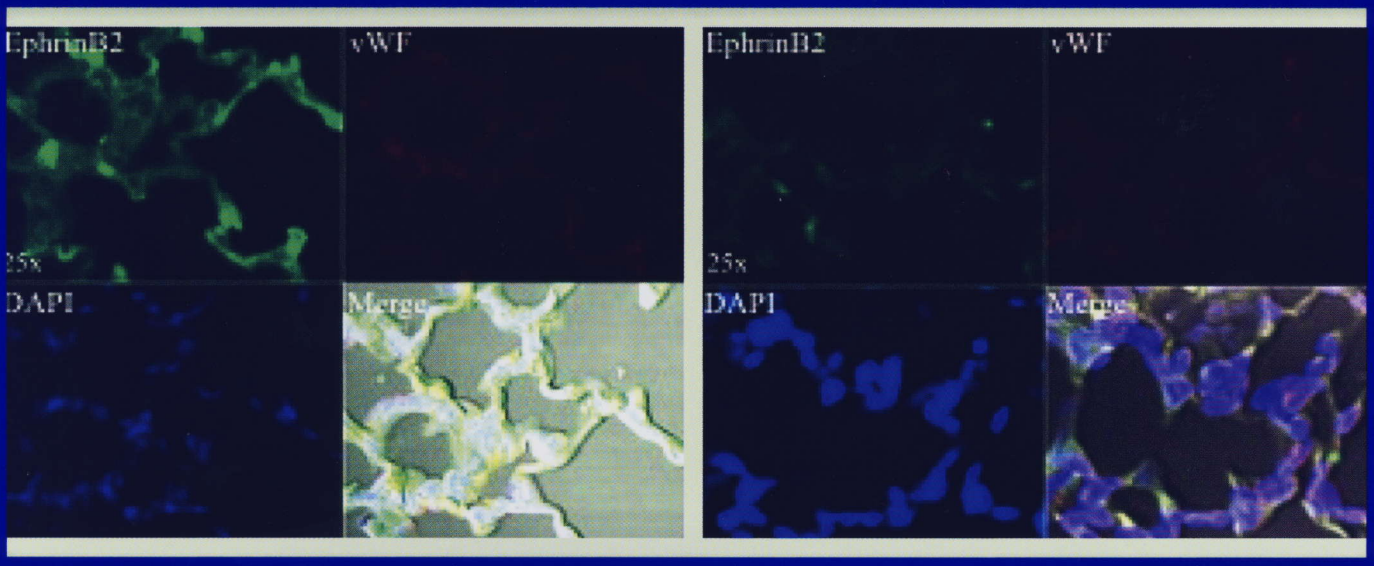

IN THIS ISSUE

ARTICLES

AN OFFICIAL JOURNAL OF THE AMERICAN THORACIC SOCIETY
Advancing Pulmonary, Critical Care, and Sleep Medicine

CONCISE CLINICAL REVIEW
Sedation and Analgesia in the Mechanically Ventilated Patient
See inside, p. 486

Critical Role of the Axonal Guidance Cue EphrinB2 in Lung Growth, Angiogenesis, and Repair

Arul Vadivel[1], Tim van Haaften[1], Rajesh S. Alphonse[1], Gloria-Juliana Rey-Parra[1], Lavinia Ionescu[1], Al Haromy[2], Farah Eaton[1], Evangelos Michelakis[2], and Bernard Thébaud[1,2,3]

[1]Department of Pediatrics, School of Human Development, Women and Children's Health Research Institute, [2]Cardiovascular Research Center, and [3]Pulmonary Research Group, University of Alberta, Edmonton, Canada

***Rationale*: Lung diseases characterized by alveolar damage currently lack efficient treatments. The mechanisms contributing to normal and impaired alveolar growth and repair are incompletely understood. Axonal guidance cues (AGC) are molecules that guide the outgrowth of axons to their targets. Among these AGCs, members of the Ephrin family also promote angiogenesis, cell migration, and organogenesis outside the nervous system. The role of Ephrins during alveolar growth and repair is unknown.**

***Objectives*: We hypothesized that EphrinB2 promotes alveolar development and repair.**

***Methods*: We used *in vitro* and *in vivo* manipulation of EphrinB2 signaling to assess the role of this AGC during normal and impaired lung development.**

***Measurements and Main Results*: *In vivo* EphrinB2 knockdown using intranasal siRNA during the postnatal stage of alveolar development in rats arrested alveolar and vascular growth. In a model of O_2-induced arrested alveolar growth in newborn rats, air space enlargement, loss of lung capillaries, and pulmonary hypertension were associated with decreased lung EphrinB2 and receptor EphB4 expression. *In vitro*, EphrinB2 preserved alveolar epithelial cell viability in O_2, decreased O_2-induced alveolar epithelial cell apoptosis, and accelerated alveolar epithelial cell wound healing, maintained lung microvascular endothelial cell viability, and proliferation and vascular network formation. *In vivo*, treatment with intranasal EphrinB2 decreased alveolar epithelial and endothelial cell apoptosis, preserved alveolar and vascular growth in hyperoxic rats, and attenuated pulmonary hypertension.**

***Conclusion*: The AGC EphrinB2 may be a new therapeutic target for lung repair and pulmonary hypertension.**

Keywords: oxygen; lung injury; angiogenesis; repair; aging

AT A GLANCE COMMENTARY

Scientific Knowledge on the Subject

Currently the mechanisms regulating alveolar growth are incompletely understood. Likewise, there is no effective preventative therapy for diseases characterized by alveolar damage. Axonal guidance cues (AGC) are molecules that guide the outgrowth of axons to their targets. AGC may play similar roles during the outgrowth of secondary crests that form the alveoli and show promise for lung repair.

What This Study Adds to the Field

The AGC EphrinB2 promotes normal alveolar growth, preserves alveolar development, and prevents pulmonary hypertension in an oxygen-induced model of arrested alveolar growth in newborn rats. EphrinB2 may have therapeutic potential for preventing alveolar damage and pulmonary hypertension.

Chronic lung diseases are projected to become the third leading cause of death by 2030 (1). Acute and chronic lung diseases, such as bronchopulmonary dysplasia (BPD) in premature infants, acute respiratory distress syndrome (ARDS), and emphysema, represent a major health care challenge because of lack of efficient therapies. A common denominator of these diseases is the absence of injury resolution, leading to distorted tissue repair and/or scarring, resulting in arrested alveolar growth in BPD, alveolar destruction in emphysema, and fibrosis in ARDS. Despite remarkable knowledge acquired over recent years in understanding the mechanisms of lung injury and repair (2), modern clinical management remains devoid of drug-based therapies promoting lung repair. Because of the suggestion that lung remodeling, repair, and regeneration recapitulate respiratory ontogeny (3), understanding how alveoli and the underlying capillaries develop and how these mechanisms are disrupted in disease states is critical for developing effective therapies for lung diseases characterized by alveolar damage.

AGCs are molecules that regulate neural network formation in the nervous system and the outgrowth of axons. During development, specific connections between neurons and between neurons and their nonneuronal targets are determined in part by guidance molecules that allow neuronal growth cones to make selective pathway choices by providing both repulsive and attractive signals (4). Emerging evidence suggest that nerves and vessels use common signaling cues to regulate their guidance (5). Blood vessels contribute to normal alveolar development and repair (reviewed in References 6 and 7). Therefore, similar mechanisms may apply to the outgrowth of secondary crests that subdivide the sacculi into alveoli to increase the gas-exchange surface area during alveolar development (8).

Among AGCs, members of the Ephrin family, EphrinB2 and its receptor EphB4, contribute to capillary bed formation (9). This finding suggests that EphrinB2 and EphB4 may be required for proper patterning of the vascular system and organ morphogenesis. Thus, AGCs are appealing candidates for the regulation of

(*Received in original form March 25, 2011; accepted in final form November 18, 2011*)

Supported by the Canadian Institutes of Health Research (CIHR). A.V. and R.S.A. are supported by a studentship from the Mazankowski Heart Institute. T.v.H. was supported by a stipend from the Maternal Fetal Neonatal Health Training Program sponsored by CIHR-IHDCYH. G.-J.R.-P. and R.S.A. are supported by the Alberta Heritage Foundation for Medical Research (AHFMR)/Alberta Innovates Health Solutions (AIHS). R.S.A. is supported by the Women and Children's Health Research Institute. B.T. is a Clinical Scholar of AHFMR/AIHS and is supported by the Canada Research Chairs Program, Canada Foundation for Innovation, and by the Stollery Children's Hospital Foundation.

Author Contributions: All authors contributed to conception and design, acquisition of data or analysis and interpretation of data, drafting the article or revising it critically, and gave their final approval of the version to be published.

Correspondence and requests for reprints should be addressed to Bernard Thébaud, M.D., Ph.D., University of Alberta, HMRC 407, Edmonton, AB, T6G 2S2 Canada. E-mail: bthebaud@ualberta.ca

This article has an online supplement, which is accessible from this issue's table of contents at www.atsjournals.org

Am J Respir Crit Care Med Vol 185, Iss. 5, pp 564–574, Mar 1, 2012
Copyright © 2012 by the American Thoracic Society
Originally Published in Press as DOI: 10.1164/rccm.201103-0545OC on December 8, 2011
Internet address: www.atsjournals.org

alveolar development and repair. Here we show that: (*1*) EphrinB2 contributes to normal postnatal alveolar development because its inhibition leads to arrested alveolar and lung vascular growth; (*2*) EphrinB2 signaling is impaired in an experimental model of O_2-induced arrested alveolar growth (mimicking features of BPD) in newborn rats; and (*3*) EphrinB2 treatment preserves alveolar and lung vascular growth and attenuates pulmonary hypertension in this model, in part by decreasing lung alveolar epithelial cell (AEC) apoptosis, improving AEC wound healing, and maintaining the ability of lung microvascular endothelial cells to proliferate and form vascular networks. Some of the results of these studies have been previously reported in the form of an abstract (10).

METHODS

Expanded methods are available in the online supplement. All procedures were approved by the Institutional Animal Care and Use Committee at the University of Alberta.

In Vivo EphrinB2 Knockdown Using Small Interfering RNA

Lung EphrinB2 was inhibited using intranasal EphrinB2 small interfering RNA (siRNA) (Ambion, Austin, TX) administration (4 μg/g in 2.5 μl/g) (11) to rat pups at postnatal day (P) 4, P7, and P10 (11–13).

Lung Endothelial Cell Isolation

Endothelial cells were isolated from P14 lungs. A single cell suspension—obtained from chopped lung pieces and strained through 70- and 40-mm cell strainers—was washed in Dulbecco's modified Eagle medium with 10% fetal calf serum, resuspended in phosphate-buffered saline containing 0.1% (w/v) bovine serum albumin, and incubated with streptavidin-tagged Dynabeads (Dynal; Invitrogen, Burlington, ON) pretreated with biotinylated anti-rat CD31 antibody (Abcam, Cambridge, MA). Dynabead-tagged CD31-positive cells were selected and snap frozen in liquid nitrogen and stored in −80°C until use.

Immunoblotting

Protein expression in whole lungs was measured with immunoblotting as previously described (14) using commercially available antibodies.

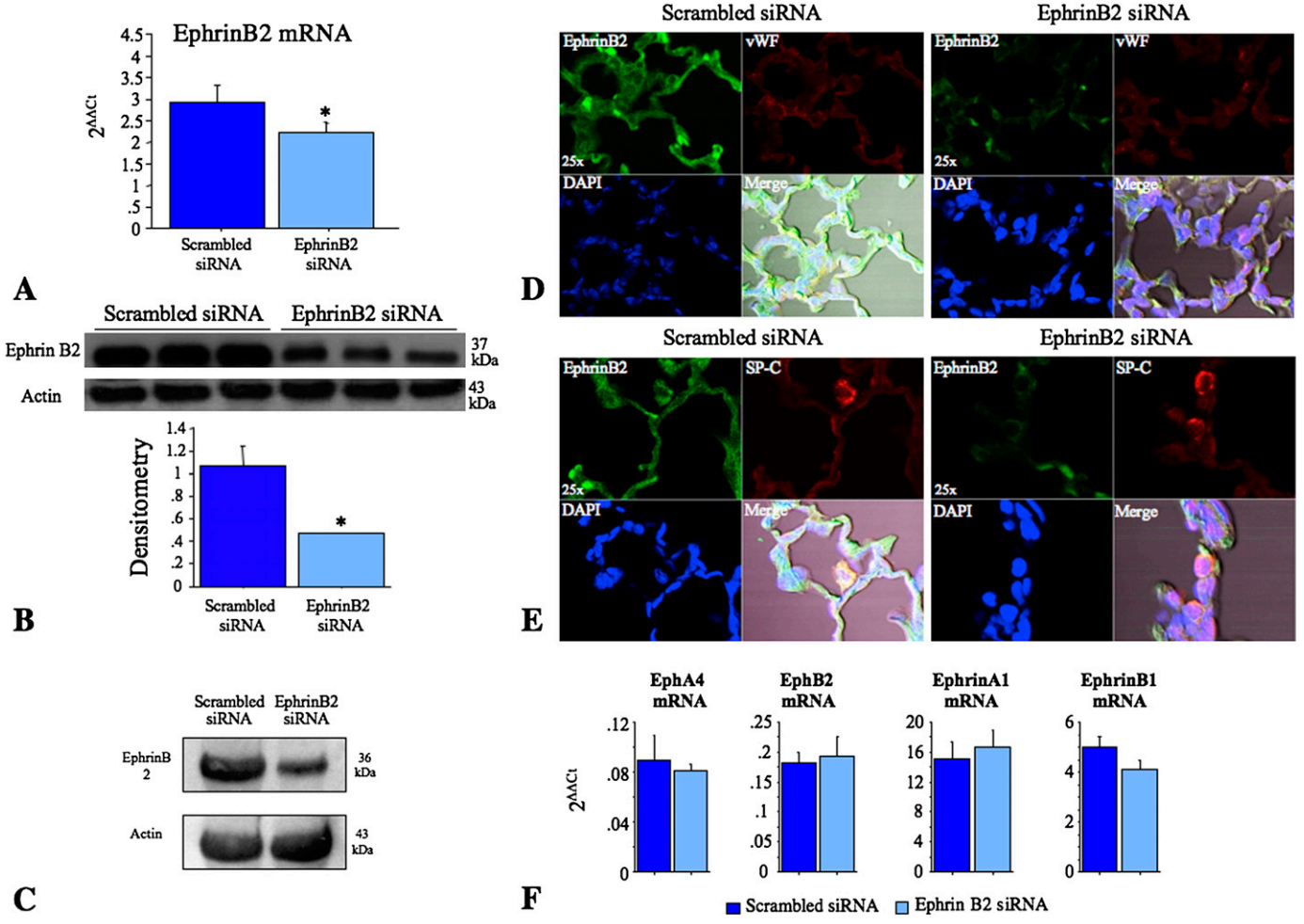

Figure 1. Intranasal EphrinB2 small interfering RNA (siRNA) results in efficient lung EphrinB2 knockdown. (*A*) Quantitative real-time–polymerase chain reaction (RT-PCR) showing decreased whole-lung EphrinB2 mRNA expression with intranasal EphrinB2 siRNA administration as compared with scrambled siRNA at P14 (n = 3 lungs per group, $*P < 0.05$). (*B*) Immunoblotting showing decreased whole-lung EphrinB2 protein expression with intranasal EphrinB2 siRNA administration as compared with scrambled siRNA at P14 (n = 3 lungs per group, $*P < 0.05$). (*C*) Immunoblotting on freshly isolated lung endothelial cells shows attenuated EphrinB2 protein expression in siRNA EphrinB2–treated lungs compared with scrambled siRNA–treated lungs at P14. Results were obtained from 12 pooled lungs per group. (*D*) Representative confocal microscopy of lung sections stained for EphrinB2 (*green*) and von Willebrand factor (vWF) (*red*). Ephrin B2 colocalizes to vWF-positive cells. EphrinB2 siRNA–treated lungs had attenuated EphrinB2 expression at P14 compared with scrambled RNA–treated lungs. (*E*) Representative confocal microscopy of lung sections stained for EphrinB2 (*green*) and surfactant protein C (SP-C) (*red*). EphrinB2 expression does not colocalize with SP-C–positive cells. (*F*) Quantitative RT-PCR showing no changes in the expression of EphA4, EphB2, EphrinA1, and EphrinB1 whole-lung mRNA expression after intranasal EphrinB2 siRNA administration as compared with scrambled siRNA at P14 (n = 3 lungs per group). DAPI = 4′,6-diamidino-2-phenylindole.

Lung Morphometry

Lungs were fixed with a 10% formaldehyde solution through the trachea at a constant pressure of 20 cm H_2O as described (14, 15). Alveolar structures were quantified on systematically sampled lung sections using the mean linear intercept (14, 15).

Barium-Gelatin Angiograms and Arterial Density Counts

Barium was infused in the main pulmonary artery as previously described (14, 15). Six animals per group, five sections per lung, and 10 high-power fields per section were counted.

Oxygen-induced Lung Injury

Experimental BPD was induced as previously described (14, 15). Sprague-Dawley rats (Charles River, Saint Constant, QC, Canada) were exposed to normoxia (21% O_2) or hyperoxia (95% O_2, BPD model) from birth to P14 in sealed Plexiglas chambers with continuous O_2 monitoring (BioSpherix, Redfield, NY).

Quantitative Real-Time Polymerase Chain Reaction

Whole lungs were analyzed by quantitative real-time polymerase chain reaction using specific primers (Applied Biosystems, Foster City, CA) as previously described (14, 15).

Immunofluorescence Using Confocal Microscopy

Immunofluorescence was performed on paraffin-embedded sections as previously described (14, 15).

Isolation and O_2 Exposure of Alveolar Epithelial Type 2 Cells

Alveolar epithelial type 2 cells (AEC2) were isolated from time-dated fetal day 19.5 rat lungs as previously described using serial differential adhesions to plastic and low-speed centrifugations (15, 16).

In Vitro AEC2 Cell Viability Assay

After 48 hours of culture in normoxic or hyperoxic conditions, cell viability was evaluated by measuring the mitochondrial-dependent reduction of colorless 3-(4,5-dimethylthiazol-2-yl)-2,5-diphenyltetrazolium bromide (MTT) (Invitrogen, Eugene, OR) as described (16).

Wound-Healing Assay with Fetal Rat AEC2

Monolayers of AEC2 (10^6 cells/ml) were scraped with a pipette tip, and the wound surface area was recorded over time with OpenLab (Quorum Technologies Inc, Guelph, ON, Canada) (15).

Isolation and Proliferation of Pulmonary Microvascular Endothelial cells

Pulmonary microvascular endothelial cells (PMVEC) were isolated from room air and hyperoxia-exposed newborn rat lungs as described by King and colleagues (17). PMVEC viability between treatment groups was compared at 72-hour intervals using the MTT assay.

Endothelial Network Formation Assay

The formation of cordlike structures by PMVEC was assessed in Matrigel-coated wells as described (14, 15).

Cell Cycle Analysis by DNA Content

Rat lung microvascular endothelial cells were stained with propidium iodide solution (Sigma-Aldrich, St. Louis, MO) in the presence of 0.1% Triton X and 0.02% DNase free RNase A (Sigma-Aldrich). Nonclumped cells were gated out and displayed with DNA area (linear red fluorescence) on the *x* axis versus cell number on the *y* axis for cell-cycle analysis using Cellquest (Beckton Dickinson, Mississauga, ON, Canada) and FlowJo (version 5.7.2) software.

In Vivo EphrinB2 Treatment

Ephrin B2/Fc (R&D Systems, Inc. Minneapolis, MN; 2 μg/200 g/d diluted in sterile distilled water) (15) was administered intranasally daily from P4 to P14.

EphrinB2 Levels

EphrinB2 levels were measured using an ELISA Kit from USCNLife (Wuhan, China).

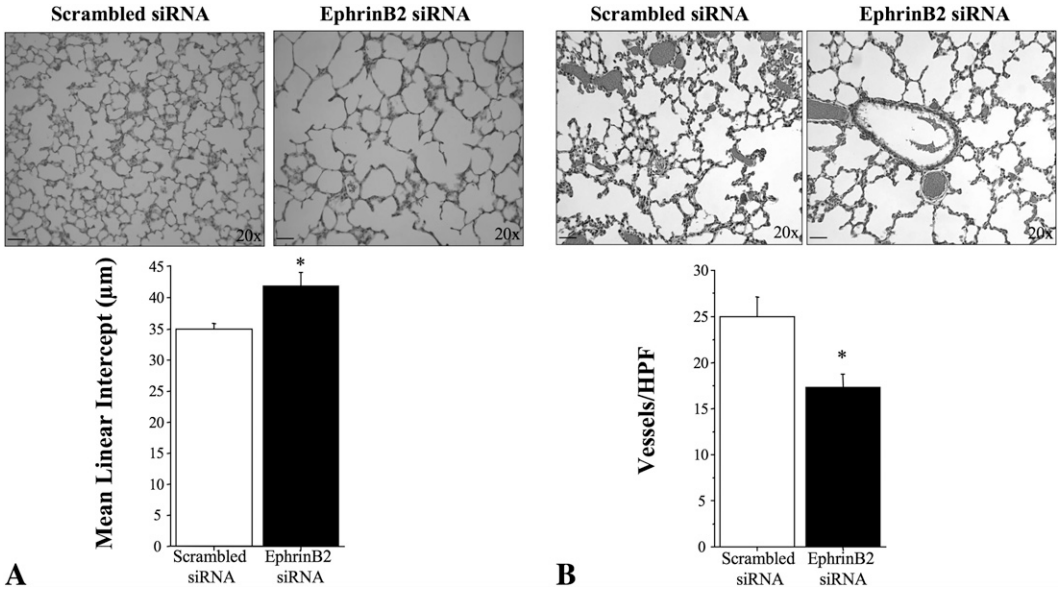

Figure 2. Intranasal EphrinB2 small interfering RNA (siRNA) results in arrested alveolar and vascular growth. (*A*) Hematoxylin and eosin (H&E)-stained lung sections and mean linear intercept assessment depicting alveolar simplification (fewer and larger alveoli with decreased secondary septa), resulting in a significantly higher mean linear intercept in the EphrinB2 siRNA–treated rat pups compared with scrambled siRNA (control)–treated animals ($n = 6$ lungs per group, $^*P < 0.05$, scale bar 130 μm). (*B*) Representative H&E-stained lung sections of barium-injected pulmonary arteries (*gray*) and mean vessel count per high power field (HPF) depicting decreased lung vessel density in EphrinB2 siRNA–treated rat pups compared with scrambled siRNA (control)–treated animals ($n = 6$ lungs per group, $^*P < 0.05$, scale bar 130 μm).

Scanning Electron Microscopy of Alveolar Structures

Scanning electron microscopy was performed as previously described (13–15).

Echo Doppler

Pulmonary artery acceleration time, expressed as a ratio over the right ventricular ejection time (PAAT/RVET), was assessed by Doppler echocardiography as previously described (18).

Right Ventricular Hypertrophy and Pulmonary Artery Remodeling

Right ventricle and left ventricle plus septum were weighed separately to determine the right ventricle to left ventricle plus septum ratio (RV/LV+S) as an index of right ventricular hypertrophy (RVH) (17). To assess pulmonary artery remodeling, the percent medial wall thickness (MWT) was calculated as (external diameter − lumen diameter)/vessel diameter (18).

Statistics

Values are expressed as the mean ± SEM. Statistical comparisons were made with the use of ANOVA. Post hoc analysis used a Fisher probable least significant difference test (Statview 5.1; Abacus Concepts, Berkeley, CA). A value of $P < 0.05$ was considered statistically significant.

RESULTS

EphrinB2 Inhibition Disrupts Normal Alveolar Development and Angiogenesis

Intranasal administration of EphrinB2 siRNA efficiently silenced total lung EphrinB2 mRNA (Figure 1A) and protein (Figure 1B) expression in the neonatal rat lung compared with scrambled siRNA. Freshly isolated lung endothelial cells from EphrinB2 siRNA–treated lungs had decreased EphrinB2 protein expression compared with endothelial cells isolated from scrambled siRNA–treated lungs (Figure 1C). Colocalization experiments showed that EphrinB2 expression localized to von Willebrand factor–positive cells (Figure 1D) but not to surfactant protein C (SP-C)–positive cells (Figure 1E). EphrinB2 signal was attenuated in EphrinB2 siRNA–treated lungs but not in scrambled siRNA–treated lungs (Figures 1D and 1E). EphrinB2 silencing did not affect the expression of EphA4, EphB2, EphrinA1, and EphrinB1 (Figure 1F).

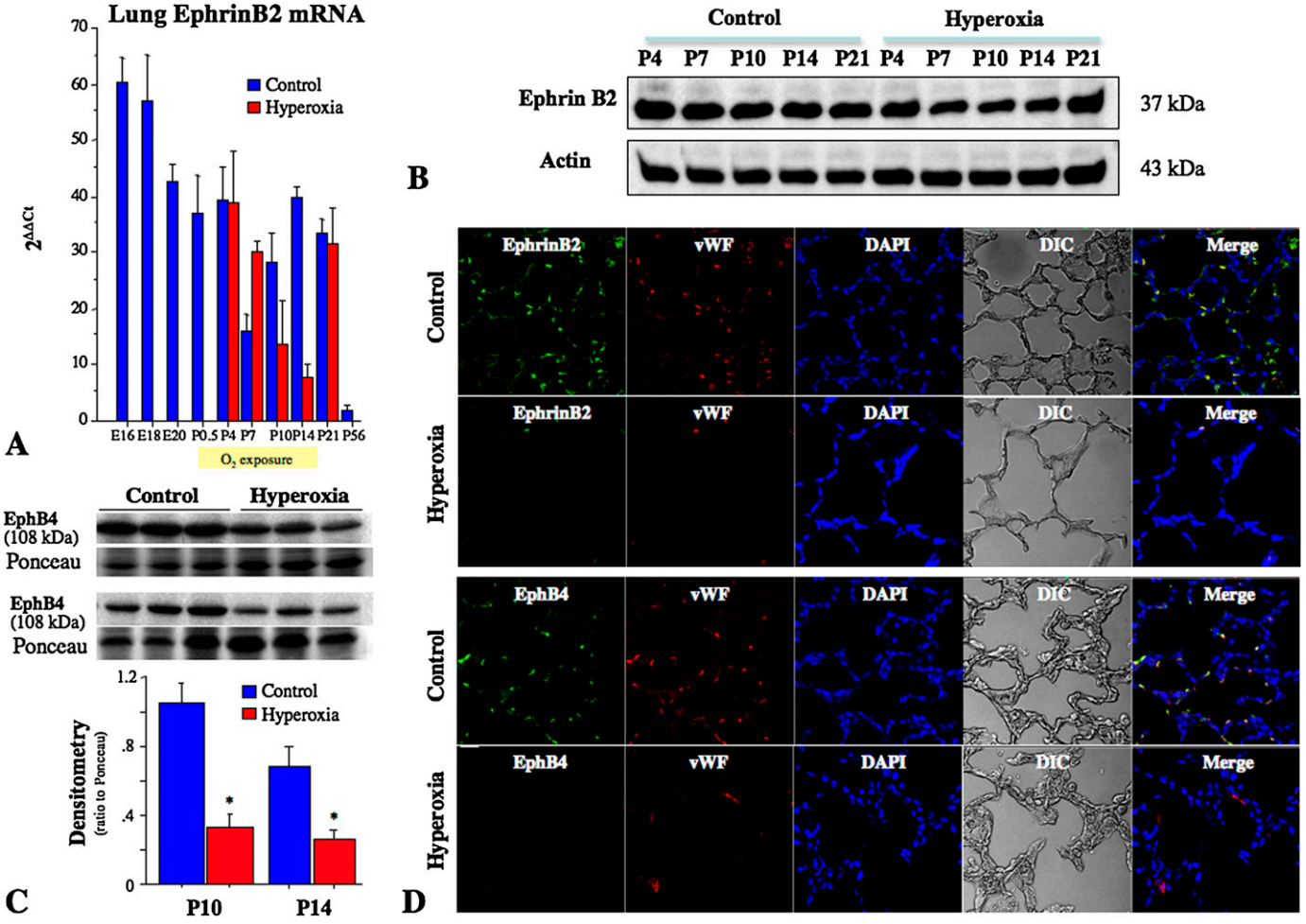

Figure 3. EphrinB2 signaling is impaired in O_2-induced arrested lung growth. (*A*) EphrinB2 mRNA expression peaks during the canalicular stage of lung development and again during late alveolar and lung microvascular development. Its expression is transiently decreased from P10 to P14 in O_2-induced experimental bronchopulmonary dysplasia (BPD) (n = 5–15 lungs per time point). (*B*). Immunoblotting showing decreased lung EphrinB2 protein expression in O_2-induced experimental BPD as compared with room air–housed control rats (each immunoblot represents n = 3 lungs per group and per time point). (*C*) Immunoblotting showing decreased lung EphB4 protein expression at P10 and P14 in O_2-induced experimental BPD as compared with room air–housed control rats (n = 3 lungs per group, $^*P < 0.05$). (*D*) Consistent with quantitative real-time–polymerase chain reaction and immunoblotting, combined immunofluorescence/confocal microscopy reveals decreased EphrinB2 and EphB4 expression in the lung of P14 rat pups with experimental O_2-induced BPD (Scale bar 65 μm). DAPI = 4′,6-diamidino-2-phenylindole; DIC = differential interference contrast; vWF = von Willebrand factor.

EphrinB2 gene silencing during the critical period of alveolar development resulted in fewer and enlarged air spaces reminiscent of BPD (Figure 2A). Decreased alveolarization was confirmed by the mean linear intercept. Impaired airspace development was associated with decreased numbers of pulmonary vessels in EphrinB2 siRNA–treated rats, as confirmed by quantification of vessel density with barium angiograms (Figure 2B). Scrambled siRNA had no effect on lung architecture and vessel growth.

Ephrin Expression during Normal Lung Development and in O_2-induced Arrested Alveolar Growth

EphrinB2 mRNA expression peaks during the canalicular stage of lung development and again during late alveolar development (Figure 3A). Its expression is transiently decreased from P10 to P14 in O_2-induced experimental BPD. This decrease was confirmed by whole-lung EphrinB2 protein expression (Figure 3B). Likewise, lung EphB4 protein expression was significantly decreased in hyperoxia compared with room air–housed rat pups (Figure 3C). Combined immunofluorescence/confocal microscopy also revealed decreased EphrinB2 and EphB4 expression in the lung of P10 and P14 rat pups with experimental O_2-induced BPD (Figure 3D).

EphrinB2 Protects AEC2 from O_2-induced Toxicity and Accelerates AEC2 Wound Healing

In vitro EphrinB2 decreased activated caspase-3 protein expression in hyperoxic AEC2 (Figure 4A), suggesting that EphrinB2 prevented lung cell apoptosis. The viability of freshly isolated AEC2, as assessed by the colorimetric MTT assay, was significantly decreased after 48 hours in 95% O_2, as compared with room air–cultured cells (Figure 4B). EphrinB2 also activated the PI3K pathway in ACE2 and prevented the O_2-induced decrease in phospho-Akt expression (Figures 4C and 4D). Recombinant

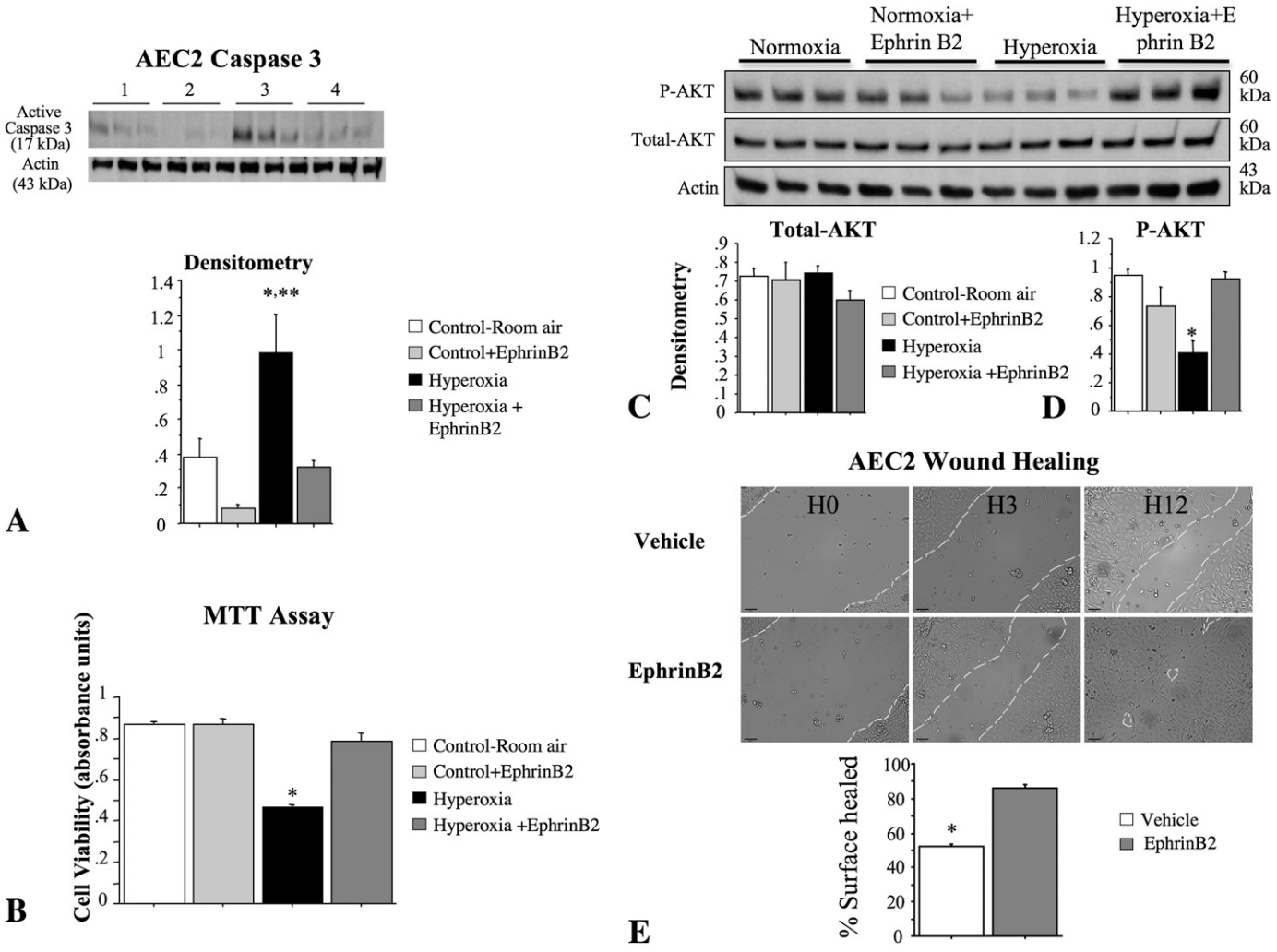

Figure 4. EphrinB2 protects type 2 alveolar epithelial cells (AEC2) from O_2-induced toxicity. (*A*) Representative immunoblot of AEC2 active caspase 3 and α-actin in the four experimental groups. Hyperoxic-exposed AEC2 had increased active caspase 3 expression, and this was attenuated by treatment with EphrinB2 (n = 3 per group, *$P < 0.01$ hyperoxia vs. control and control + EphrinB2; **$P < 0.001$ hyperoxia versus hyperoxia + EphrinB2). (*B*) AEC2 were cultured for 48 hours in room air (normoxic control) or 95% hyperoxia. Mean data of cell viability as assessed by measuring the mitochondrial-dependent reduction of colorless 3-(4,5-dimethylthiazol-2-yl)-2,5-diphenyltetrazolium bromide (MTT) shows that hyperoxia significantly decreases AEC2 viability as compared with room air–exposed cells. EphrinB2 treatment significantly improves AEC2 viability in hyperoxia (n = 5, *$P < 0.0001$). (*C* and *D*) Representative immunoblot Akt and P-Akt expression in AEC2. Hyperoxic-exposed AEC2 showed decreased P-Akt expression, which was preserved in EphrinB2-treated AEC2 (n = 3 per group, *$P < 0.05$ vs. other groups). (*E*) Confluent monolayers of AEC2 were damaged using a pipette tip, washed to remove damaged cells, and treated with vehicle or EphrinB2. EphrinB2 accelerated AEC2 wound closure as compared with vehicle (n = 6 per group, *$P < 0.0001$, scale bar 65 μm).

EphrinB2 peptide significantly enhanced AEC2 survival in hyperoxia. Finally, EphrinB2 treatment accelerated AEC2 wound healing in an *in vitro* wound healing scratch assay (Figure 4E).

EphrinB2 Protects PMVEC from O_2-induced Toxicity and Preserves Vascular Network Formation *In Vitro*

The viability of PMVECs, assessed by a colorimetric MTT assay, was significantly decreased in hyperoxia as compared with the PMVECs isolated from room air–housed rats (Figure 5A). PMVECs from EphrinB2-treated animals showed significantly increased survival in comparison with hyperoxia-exposed untreated groups. Hyperoxia also decreased the number of rat lung microvascular endothelial cells in S-phase and EphrinB2 treatment attenuated this decrease (Figure 5B).

Freshly isolated PMVECs were exposed to room air or 95% O_2 in serum-free Matrigel and assessed for the formation of vessel-like networks. Hyperoxia significantly decreased endothelial cordlike structure formation, whereas EphrinB2 significantly counteracted the effect of O_2 and promoted endothelial network formation (Figure 5C).

Intranasal Delivery of EphrinB2 Prevents Apoptosis and Preserves Alveolar and Vascular Development in Irreversible O_2-induced BPD

Intranasal delivery of EphrinB2 resulted in significantly higher levels of EphrinB2 in lung homogenates compared with untreated lungs (0.56 vs. 0.42 ng/ml, $P < 0.02$, n = 6 per group). Caspase 3 expression was increased in SP-C– (Figure 6A) and PECAM- (Figure 6B) positive cells in the lung of hyperoxic rat pups. Intranasal delivery of EphrinB2 attenuated caspase 3 expression in both cell types as confirmed by semiquantitative analysis (Figures 6C and 6D). Likewise, whole-lung caspase 3 was increased in hyperoxic rat pups, which was attenuated by EphrinB2 treatment (Figure 6E).

Hyperoxia induced a histological pattern reminiscent of human BPD, characterized by airspace enlargement with simplified and fewer alveolar structures as shown on representative hematoxylin and eosin–stained sections (Figure 7A) and representative scanning electron microscopy sections (Figure 7B). Intranasal administration of EphrinB2 from P4 to P14 preserved alveolar development as quantified by the mean linear intercept (Figure 7C).

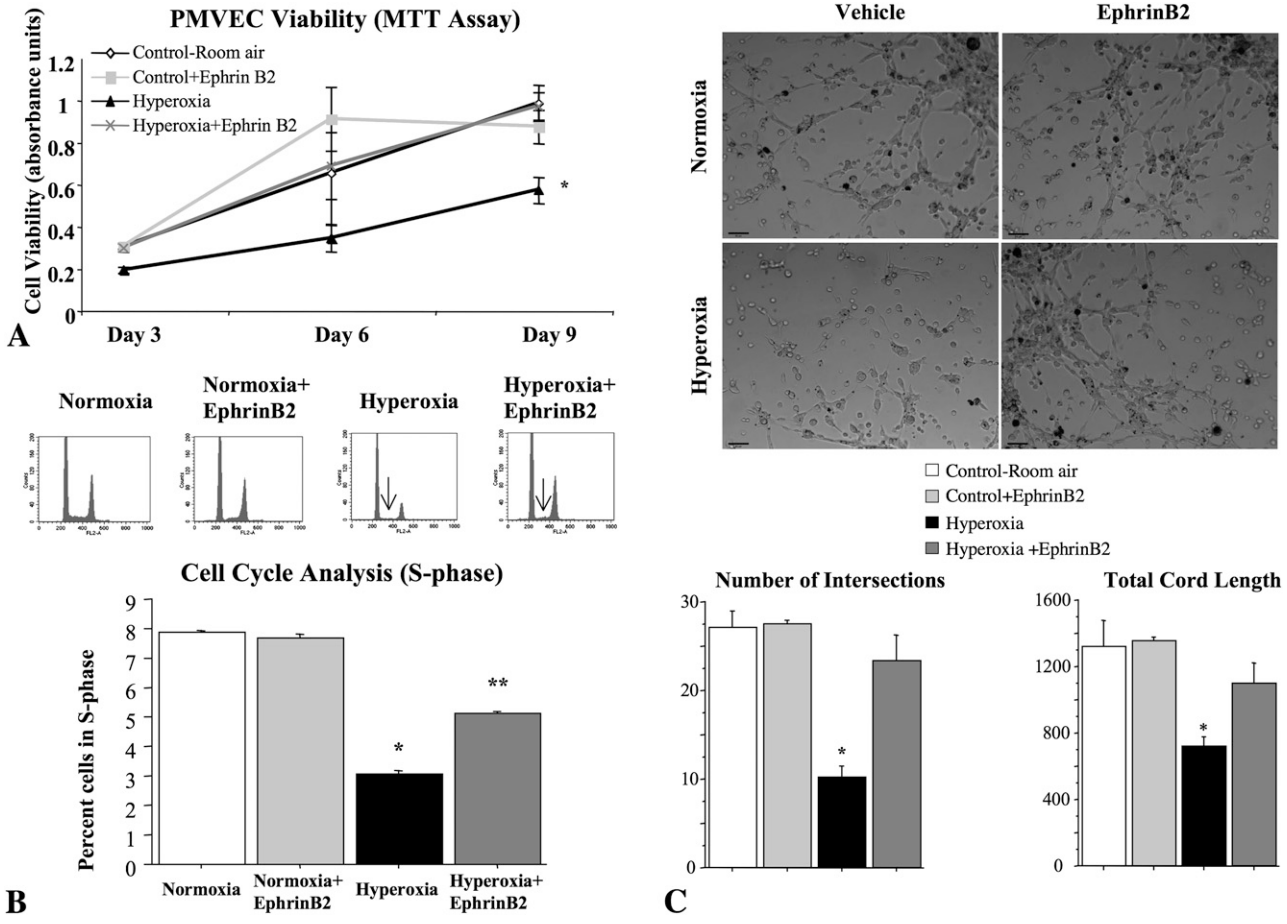

Figure 5. EphrinB2 protects pulmonary microvascular endothelial cells (PMVEC) from O_2-induced toxicity. (*A*) PMVEC viability. PMVECs isolated at P14 from lungs of the four treatment groups were seeded in 48-well cell culture plates at a density of 10^4 cells/well and allowed to attach over 24 hours. After medium change on Day 2, the cells were allowed to grow for 9 days and their viability was evaluated at 72-hour intervals by a 3-(4,5-dimethylthiazol-2-yl)-2,5-diphenyltetrazolium bromide (MTT) assay. Mean data of cell viability shows that the cells isolated from the hyperoxia group had significantly lower viability as compared with the cells isolated from room air groups. The cells isolated from the EphrinB2-treated groups had significantly higher viability than PMVECs from untreated hyperoxic lungs (n = 5 per group, $*P < 0.0001$ hyperoxia vs. other groups). (*B*) Cell cycle analysis by DNA content. Representative figures of flow cytometry and mean data showing that hyperoxia decreased the number of rat lung microvascular endothelial cells in the S-phase. EphrinB2 treatment attenuated this decrease (n = 3 lungs per group, $*P < 0.001$). (*C*) EphrinB2 promotes endothelial network formation. Quantitative assessment of cordlike structure formation shows a significant decrease in the number of intersects and the total length of cordlike structures in hyperoxia. EphrinB2 preserved the number of intersects and total cord-structure length. (n = 3 per group, $*P < 0.05$ hyperoxia vs. other groups, scale bar 65 μm).

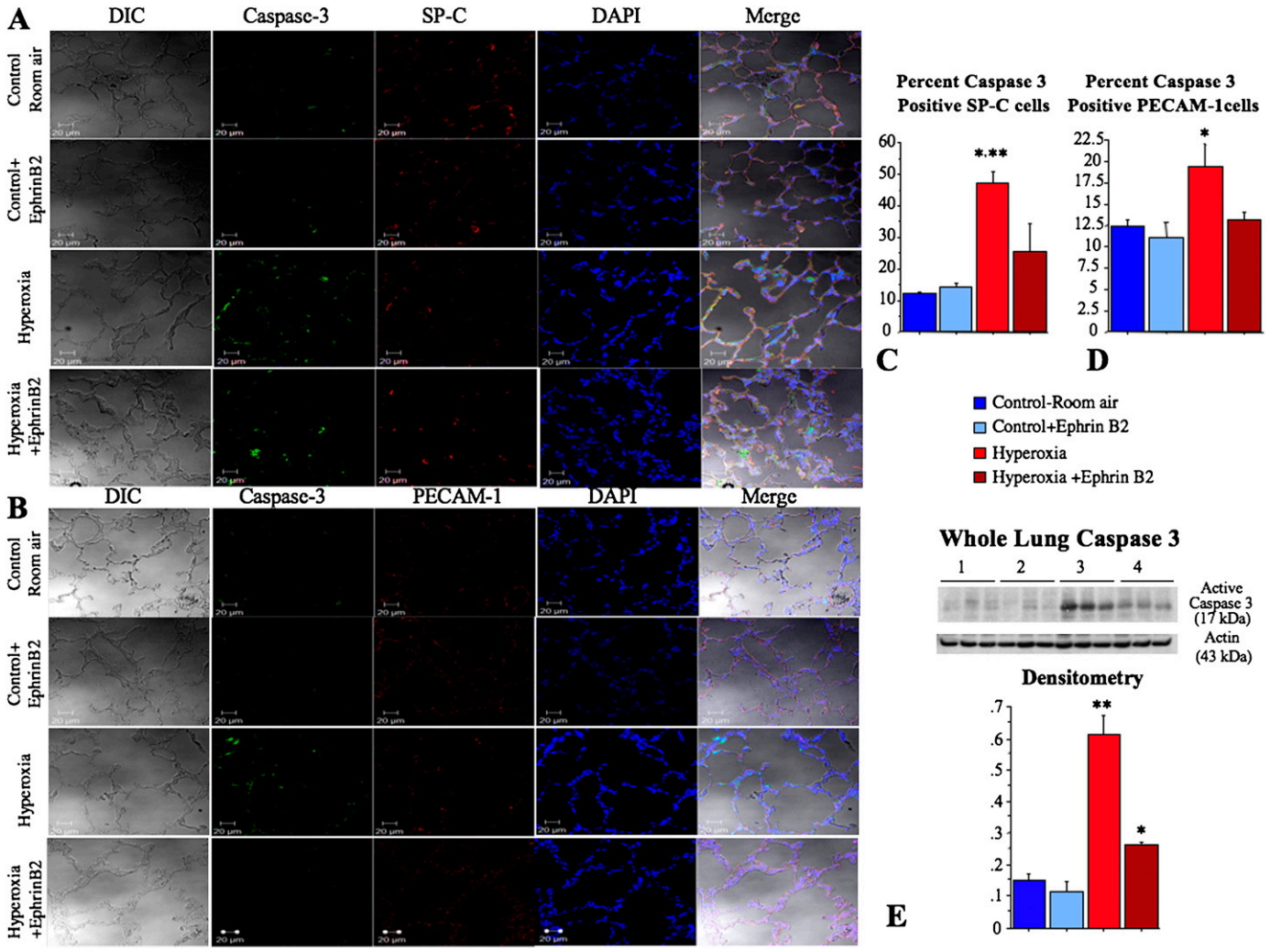

Figure 6. *In vivo* EphrinB2 treatment prevents alveolar epithelial and endothelial cell apoptosis in experimental O_2-induced bronchopulmonary dysplasia. (*A*) Representative confocal microscopy of lung sections stained for caspase 3 and surfactant protein C (SP-C). (*B*) Representative confocal microscopy of lung sections stained for caspase 3 and platelet endothelial cell adhesion molecule (PECAM). (*C*) Mean data showing increased caspase 3 expression in SP-C–positive cells in hyperoxia that is attenuated by EphrinB2 (n = 3 lungs per group, $*P < 0.005$ hyperoxia vs. normoxia and normoxia + EphrinB2, $**P < 0.05$ hyperoxia vs. hyperoxia + EphrinB2). (*D*) Mean data showing increased caspase 3 expression in PECAM-1–positive cells in hyperoxia that is attenuated by EphrinB2 (n = 3 lungs per group, $*P < 0.05$, hyperoxia vs. other groups). (*E*) Representative immunoblot of whole-lung active caspase 3 and α-actin in the four experimental groups. Lungs of hyperoxic-exposed rat pups showed increased active caspase 3 expression, and this was attenuated by treatment with EphrinB2 (n = 3 per group, $*P < 0.02$ hyperoxia + EphrinB2 vs. normoxia + EphrinB2, $**P < 0.0001$ vs. other groups). DAPI = 4′,6-diamidino-2-phenylindole; DIC = differential interference contrast.

EphrinB2 treatment had no adverse effects on lung architecture in control animals.

Arrested lung vascular growth is another hallmark of BPD. Hyperoxic exposure caused a severe decrease in pulmonary vessel density, as quantified on barium angiograms (Figures 8A and 8B). EphrinB2-treated rat pups had higher pulmonary vessel density than untreated hyperoxic rat pups (Figures 8A and 8B). EphrinB2 treatment had no adverse effects on lung angiogenesis in control animals.

EphrinB2 Reduced Pulmonary Hypertension Associated with O_2-induced Lung Injury

Pulmonary hypertension is a significant complication in severe BPD and other chronic lung diseases (19–21). Chronic exposure to hyperoxia was associated with a significant decrease in the PAAT/RVET (Figure 9A) and an increase in RVH (Figure 9B) and MWT of small pulmonary arteries (Figure 9C). EphrinB2 attenuated these functional and structural features of pulmonary hypertension as indicated by the increase in mean PAAT/RVET (Figure 9A), reduction in RV/LV+S (Figure 9B), and decrease in MWT (Figure 9C).

DISCUSSION

We demonstrate that EphrinB2 is critical for normal alveolar growth and repair: *in vivo* EphrinB2 inhibition during the period of alveolar development arrests alveolar and lung vascular growth, resulting in histological changes reminiscent of BPD. Likewise, in experimental O_2-induced BPD, arrested alveolar and vascular growth is associated with disrupted EphrinB2 signaling. Conversely, treatment with recombinant EphrinB2 protects AEC2 and PMVEC from O_2 toxicity and accelerates AEC2 wound healing *in vitro*. *In vivo*, EphrinB2 administration preserves alveolar and lung vascular growth and alleviates echographic and structural signs of pulmonary hypertension.

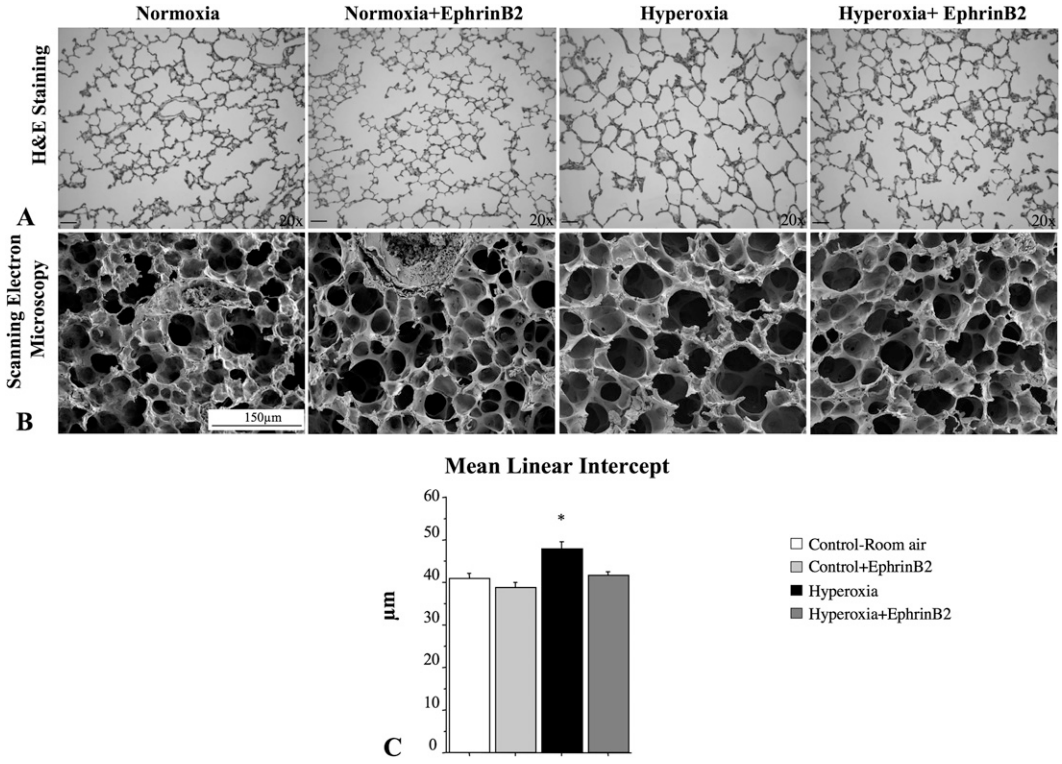

Figure 7. Representative (*A*) hematoxylin and eosin (H&E)-stained (scale bar 130 μm) and (*B*) scanning electron microscopy (scale bar 150 μm) lung sections at P21 showing larger and fewer alveoli in hyperoxia-exposed lungs as compared with lungs of normoxic-housed rat pups. Treatment of hyperoxia-exposed animals with EphrinB2 preserved alveolar structure. (*C*) The mean linear intercept confirms arrested alveolar growth in untreated O_2-exposed animals and preserved alveolar structure with EphrinB2 treatment (n = 5 per group, $^*P < 0.05$ hyperoxia vs. other groups).

This is the first observation suggesting a lung-protective effect of AGC.

Pivotal Role for the AGC EphrinB2 during Alveolar Development

In contrast to the large amount of information regarding the genetic control of the dichotomous division of the conducting airways in mammals, derived from studies of the respiratory system in *Drosophila* (22), much less is known about the mechanisms that regulate alveolar development. The genetic control of alveolarization remains poorly understood, mainly because of the lack of alveoli in *Drosophila*. Furthermore, the conducting airways grow into the surrounding mesenchyme, whereas alveolar septa evaginate inward into the air space (23). One interesting theory is that a repulsive signal pushes the septa inward (8). AGCs are appealing candidates in guiding the growth of alveolar septa in the lung during alveolar development, because they (*1*) guide axonal outgrowth through repulsion and attraction, (*2*) guide angiogenic network formation, and (*3*) promote early lung branching morphogenesis. During development, specific connections between neurons and between neurons and their nonneuronal targets are determined in part by guidance molecules that allow

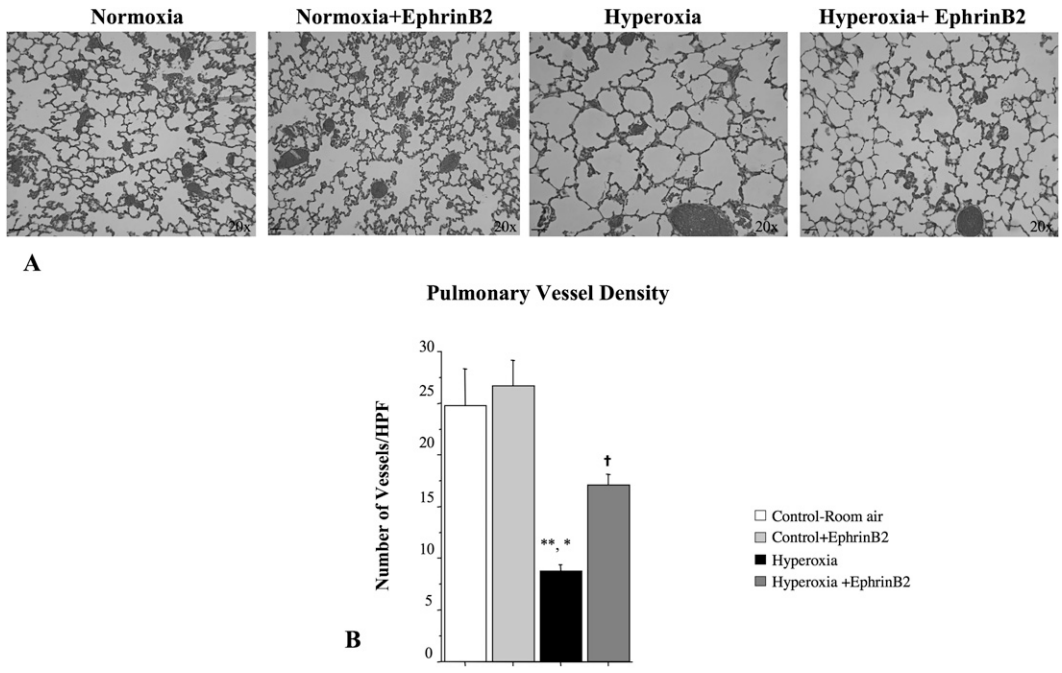

Figure 8. EphrinB2 preserves lung vessel density in O_2-induced bronchopulmonary dysplasia. (*A*) Representative hematoxylin and eosin–stained lung sections of barium-injected pulmonary arteries depicting decreased lung vessel density in hyperoxia-exposed lungs as compared with normoxia-housed rat pups and enhanced lung vessel density with EphrinB2 treatment (scale bar 130 μm). (*B*) Mean vessel count per high-power field (HPF) confirms decreased lung vessel density in untreated O_2-exposed animals. Treatment with EphrinB2 attenuated decreased lung vessel density in O_2-exposed animals. (n = 5 per group, $^{**}P < 0.001$ hyperoxia vs. normoxic groups, $^*P < 0.05$ hyperoxia vs. hyperoxia + EphrinB2, $^{\dagger}P < 0.05$ hyperoxia + EphrinB2 vs. normoxic groups).

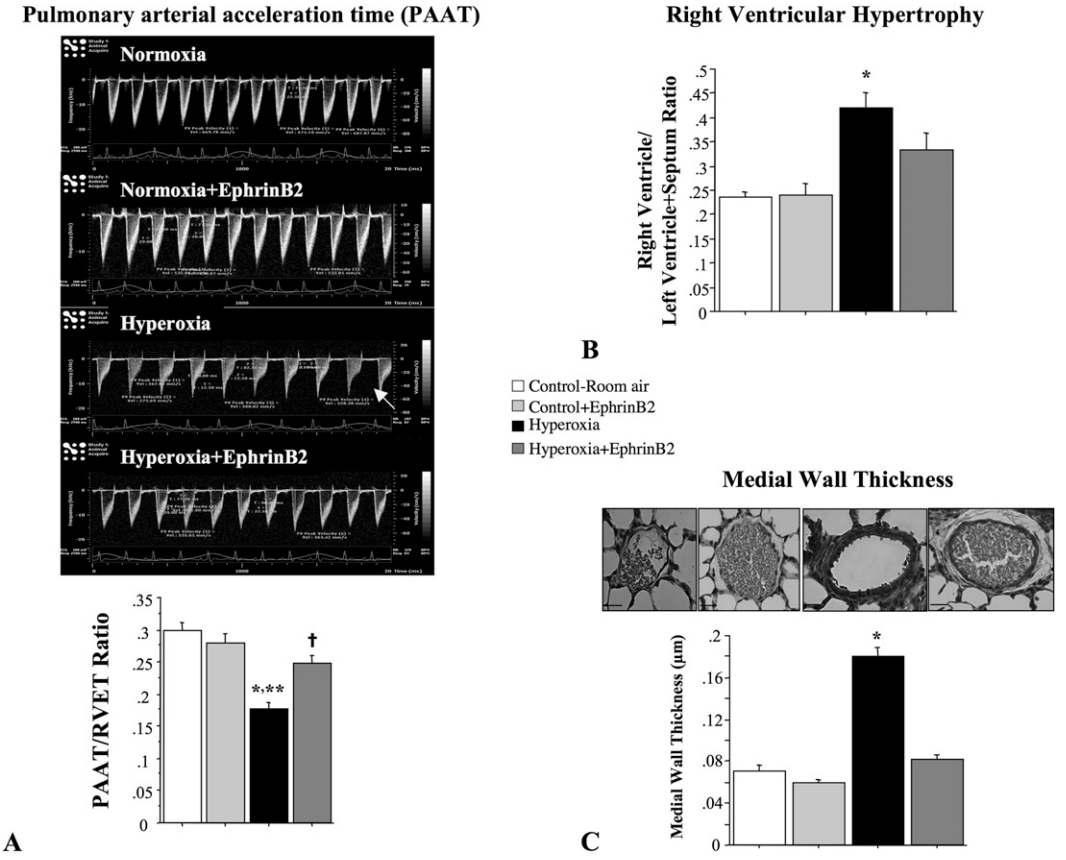

Figure 9. EphrinB2 prevents pulmonary hypertension associated with O_2-induced bronchopulmonary dysplasia. (*A*) Pulmonary arterial acceleration time/right ventricular ejection time (PAAT/RVET). Representative echo Doppler and mean PAAT/RVET showing a characteristic notch indicating pulmonary hypertension (*arrow*) in hyperoxic-exposed rat pups and a significantly decreased PAAT/RVET as compared with rat pups housed in normoxia. EphrinB2 significantly increased PAAT/RVET as compared with untreated hyperoxic rat pups ($n = 5$ animals per group, $^{**}P < 0.001$ hyperoxia vs. normoxic groups, $^{*}P < 0.01$ hyperoxia vs. hyperoxia + EphrinB2, $^{\dagger}P < 0.05$ hyperoxia + EphrinB2 vs. normoxia). (*B*) Right ventricular hypertrophy (RVH). Hyperoxic-exposed rats had significant RVH as indicated by the increase in RV/LV+S ratio compared with normoxic control rats. EphrinB2 significantly reduced RVH ($n = 5$ animals per group, $^{*}P < 0.05$). (*C*) Pulmonary arterial medial wall thickness (MWT). Representative hematoxylin and eosin–stained sections of pulmonary arteries from the four experimental groups and % mean MWT. Hyperoxic-exposed rats had a significant increase in %MWT as compared with room air–housed rat pups. EphrinB2 significantly reduced %MWT ($n = 5$ animals per group, $^{*}P < 0.05$, scale bar 65μm).

neuronal growth cones to make selective pathway choices by providing both repulsive and attractive signals. Adhesion receptors transduce the signals from the extracellular substrate to the cytoskeleton, thereby providing the traction necessary to move the growth cone, whereas guidance cues supply the directional information through attraction or repulsion (4). Emerging evidence suggests that nerves and vessels use common signaling cues to regulate their guidance (5). In the developing mouse retina, specialized tip cells located at the extremities of capillary sprouts regulate the extension of capillary sprouts in response to retinal astrocyte-derived vascular endothelial growth factor (VEGF) gradients (24), a factor that we and other have shown to be crucial for alveolar growth and repair (14, 25). Tip cells are highly similar to axonal growth cones, as they extend numerous filopodia that explore their environment. Similar mechanisms may apply to the outgrowth of secondary septa during the formation of the alveolar capillary bed and the alveoli. Increasing evidence suggests that lung blood vessels actively promote normal alveolar growth during development and contribute to the maintenance of alveolar structures throughout postnatal life (reviewed in References 6 and 7). Ephrins contribute to vascular development (9, 26, 27) and lung capillary bed formation (28, 29) and as such represent appealing candidates promoting alveolarization.

To overcome the embryonic lethality of EphrinB2 knockout mice to study the role of this AGC during postnatal alveolar development, we administered intranasal siRNA to neonatal rats to specifically silence lung EphrinB2 during the critical period of postnatal alveolar development. This strategy effectively silenced lung EphrinB2 (Figure 1) and resulted in arrested alveolar and lung vascular growth (Figure 2). This is consistent with recent findings in mice homozygous for the hypomorphic knock-in allele *ephrinB2*$^{\Delta V/\Delta V}$, encoding mutant ephrinB2 with a disrupted C-terminal PDZ interaction motif. These mice die by 2 weeks of age and have enlarged airspaces, suggesting a crucial role for EphrinB2 during alveolar development (30). Interestingly, EphrinB2 and EphB4 are also expressed in myoepithelial and epithelial cells in the mammary gland—another organ containing alveolar structures (31). In transgenic mice overexpressing EphB4 in the mammary epithelium, unscheduled expression delays development of the mammary epithelium at puberty and during pregnancy. During pregnancy, fewer lobules are formed. These, however, exhibit more numerous but smaller alveolar units, suggesting a role for EphB4 in the regulation of tissue architecture (32).

We provide additional evidence for the role of EphrinB2 during alveolar development by showing that EphrinB2 mRNA expression peaks during the canalicular stage of lung development (E16-E20)—when most of the blood vessels form in the lung—and again during the late alveolar stage of lung development, which overlaps with lung microvascular development (P10–P21) (Figure 3A). Conversely, Ephrin signaling is disrupted in O_2-induced arrested alveolar and vascular growth: EphrinB2 mRNA and protein expression are transiently decreased from P10 to P14 (Figures 3A and 3B), and lung EphB4 protein expression is also decreased in rat pups with experimental O_2-induced BPD compared with normoxic rat pups (Figure 3C). Interestingly, EphrinB2 expression is not decreased at P4 and P21 (10 d after the O_2 insult was stopped). We speculate that at P4, the injury

has not yet affected EphrinB2 expression, whereas at P21, there is a "catch up" effect to restore alveolarization. Immunofluorescence also shows that EphrinB2 expression is reduced in hyperoxic lungs, although the loss of EphrinB2 expression could simply reflect the vascular pruning and loss of endothelial cells because EphrinB2 colocalizes to PECAM-1–positive cells (Figure 3D).

The AGC EphrinB2 Promotes Alveolar Repair

Altogether, these observations suggest that EphrinB2 promotes normal alveolar development and formed the rationale for testing the therapeutic potential of EphrinB2 to preserve normal alveolar development in a model of O_2-induced arrested alveolar growth. Here we show, both *in vitro* and *in vivo*, that EphrinB2 indeed exerts lung-protective properties.

In vitro, EphrinB2 prevented ACE2 apoptosis and preserved AEC2 viability in hyperoxia through activation of the PI3K pathway. EphrinB2 also accelerated AEC2 wound closure (Figure 4), suggesting that EphrinB2 promotes wound healing. This is consistent with up-regulated EphrinB2 expression in both perilesional and lesional intestinal epithelial cells of patients with inflammatory bowel disease, and recombinant EphB1-Fc enhanced wound closure of rat intestinal epithelial cells (33).

Because angiogenesis promotes alveolar growth (6, 7), we demonstrate that EphrinB2 promotes PMVEC proliferation and maintains PMVEC network formation in hyperoxia (Figure 5). Accordingly, previous findings report that ephrin-B2/EphB signaling and EphB4 receptor stimulation increase migration of endothelial cells via the PI3 kinase pathway, thereby contributing to neovascularization in adulthood (34, 35).

Whether inhibition of vascular growth may be a cause or consequence of impaired alveolarization remains controversial. Nonetheless, we and others showed the therapeutic potential for angiogenic growth factor modulation in lung diseases characterized by alveolar damage (12, 24), and our *in vitro* data provided strong rationale for the lung-protective effect of EphrinB2. To explore EphrinB2's therapeutic potential *in vivo*, we used the hyperoxic BPD model of lung injury, hypothesizing that EphrinB2 would promote lung angiogenesis and thereby stimulate alveolarization. In the present study, we chose the intranasal route to mimic the clinical setting wherein exogenous surfactant is routinely administered to premature infants with respiratory distress and at risk of developing BPD (36). Hence, concomitant administration of lung-protective agents with surfactant through the endotracheal tube in critically ill patients is appealing and clinically relevant. Consistent with our *in vitro* data, EphrinB2 preserved alveolar growth and lung angiogenesis in hyperoxic-exposed pups, suggesting EphrinB2 as new therapeutic target to prevent alveolar damage.

The AGC EphrinB2 Prevents Pulmonary Hypertension

Pulmonary hypertension often complicates chronic lung diseases, including BPD (20), pulmonary fibrosis (19), and emphysema (18), and significantly worsens the prognosis. Few studies have shown beneficial hemodynamic and structural effects of EphrinB2 in animal models of myocardial and hind limb ischemia (37, 38), but the effect of EphrinB2 on pulmonary hypertension has never been investigated. The hyperoxic BPD model in rats exhibits marked pulmonary hypertension as assessed by echo Doppler (decreased PAAT/RVET), RVH, and remodeling of the pulmonary arteries. EphrinB2 alleviated pulmonary hypertension in this model, warranting further studies in other models of pulmonary hypertension. The mechanism by which EphrinB2 attenuates pulmonary hypertension, besides increasing lung angiogenesis, remains unclear. In this model, decreased NO signaling, excessive reactive oxygen species, and endothelin pathway activation contribute to pulmonary hypertension (39). To our knowledge, there are no data available on Ephrin interactions with these signaling pathways. Conversely, the proangiogenic function of EphrinB2 has been linked to a role in the VEGF signaling pathway. Hyperoxia exposure is known to suppress VEGF expression in newborn rats (14), and VEGF promotes lung microvascular regeneration in adult rats (40) and neonatal hyperoxic rats (14) with pulmonary hypertension. Recent reports show that activation of Ephrin B2 reverse signaling leads to transient association with VEGFR-2 and VEGFR-3 and promotes endocytosis, thereby enhancing VEGF receptor signaling inside the cell (41, 42). Thereby, Ephrin B2 promotes VEGF function to enhance VEGF-mediated angiogenesis. Interestingly also, EphrinB2 expression is up-regulated in adult endothelial cells during arterial remodeling, controlled by cyclic stretch, and EphrinB2 limits smooth muscle cell migration (43), a hallmark of pulmonary hypertension.

In conclusion, we confirm that the AGC EphrinB2 is necessary for normal alveolar development. In addition, we show that EphrinB2 exerts therapeutic benefit in protecting the lung from O_2-induced alveolar injury and pulmonary hypertension. Our data offer new therapeutic options for lung diseases characterized by alveolar damage and pulmonary hypertension.

Author disclosures are available with the text of this article at www.atsjournals.org

References

1. World Health Organization. The global burden of disease: 2004 update. Geneva, World Health Organization. 2004.
2. Martin TR. Interactions between mechanical and biological processes in acute lung injury. *Proc Am Thorac Soc* 2008;5:291–296.
3. Warburton D, Tefft D, Mailleux A, Bellusci S, Thiery JP, Zhao J, Buckley S, Shi W, Driscoll B. Do lung remodeling, repair, and regeneration recapitulate respiratory ontogeny? *Am J Respir Crit Care Med* 2001;164: S59–S62.
4. Barallobre MJ, Pascual M, Del Rio JA, Soriano E. The netrin family of guidance factors: emphasis on netrin-1 signalling. *Brain Res Brain Res Rev* 2005;49:22–47.
5. Carmeliet P, Tessier-Lavigne M. Common mechanisms of nerve and blood vessel wiring. *Nature* 2005;436:193–200.
6. Stenmark KR, Abman SH. Lung vascular development: implications for the pathogenesis of bronchopulmonary dysplasia. *Annu Rev Physiol* 2005;67:623–661.
7. Thebaud B, Abman SH. Bronchopulmonary dysplasia: where have all the vessels gone? Roles of angiogenic growth factors in chronic lung disease. *Am J Respir Crit Care Med* 2007;175:978–985.
8. Prodhan P, Kinane TB. Developmental paradigms in terminal lung development. *Bioessays* 2002;24:1052–1059.
9. Adams RH, Wilkinson GA, Weiss C, Diella F, Gale NW, Deutsch U, Risau W, Klein R. Roles of ephrinB ligands and EphB receptors in cardiovascular development: demarcation of arterial/venous domains, vascular morphogenesis, and sprouting angiogenesis. *Genes Dev* 1999; 13:295–306.
10. Vadivel A, Rey-Parra G, Eaton F, Thebaud B. The axonal guidance cue Ephrin promotes alveolar development. *Am J Respir Crit Care Med* 2009;179:A4106.
11. Bitko V, Musiyenko A, Shulyayeva O, Barik S. Inhibition of respiratory viruses by nasally administered siRNA. *Nat Med* 2005;11:50–55.
12. Massaro D, Massaro GD, Clerch LB. Noninvasive delivery of small inhibitory RNA and other reagents to pulmonary alveoli in mice. *Am J Physiol Lung Cell Mol Physiol* 2004;287:L1066–L1070.
13. Vadivel A, Abozaid S, van Haaften T, Sawicka M, Eaton F, Chen M, Thebaud B. Adrenomedullin promotes lung angiogenesis, alveolar development, and repair. *Am J Respir Cell Mol Biol* 2010;43:152–160.
14. Thebaud B, Ladha F, Michelakis ED, Sawicka M, Thurston G, Eaton F, Hashimoto K, Harry G, Haromy A, Korbutt G, *et al*. Vascular endothelial growth factor gene therapy increases survival, promotes lung angiogenesis, and prevents alveolar damage in hyperoxia-induced lung injury: evidence that angiogenesis participates in alveolarization. *Circulation* 2005;112:2477–2486.

15. van Haaften T, Byrne R, Bonnet S, Rochefort GY, Akabutu J, Bouchentouf M, Rey-Parra GJ, Galipeau J, Haromy A, Eaton F, *et al*. Airway delivery of mesenchymal stem cells prevents arrested alveolar growth in neonatal lung injury in rats. *Am J Respir Crit Care Med* 2009;180:1131–1142.
16. Alphonse RS, Vadivel A, Coltan L, Eaton F, Barr AJ, Dyck JR, Thebaud B. Activation of Akt protects alveoli from neonatal oxygen-induced lung injury. *Am J Respir Cell Mol Biol* 2011;44:146–154.
17. King J, Hamil T, Creighton J, Wu S, Bhat P, McDonald F, Stevens T. Structural and functional characteristics of lung macro- and microvascular endothelial cell phenotypes. *Microvasc Res* 2004;67: 139–151.
18. Ladha F, Bonnet S, Eaton F, Hashimoto K, Korbutt G, Thebaud B. Sildenafil improves alveolar growth and pulmonary hypertension in hyperoxia-induced lung injury. *Am J Respir Crit Care Med* 2005;172: 750–756.
19. Chaouat A, Naeije R, Weitzenblum E. Pulmonary hypertension in COPD. *Eur Respir J* 2008;32:1371–1385.
20. Farkas L, Farkas D, Ask K, Moller A, Gauldie J, Margetts P, Inman M, Kolb M. VEGF ameliorates pulmonary hypertension through inhibition of endothelial apoptosis in experimental lung fibrosis in rats. *J Clin Invest* 2009;119:1298–1311.
21. Mourani PM, Ivy DD, Gao D, Abman SH. Pulmonary vascular effects of inhaled nitric oxide and oxygen tension in bronchopulmonary dysplasia. *Am J Respir Crit Care Med* 2004;170:1006–1013.
22. Metzger RJ, Krasnow MA. Genetic control of branching morphogenesis. *Science* 1999;284:1635–1639.
23. Roth-Kleiner M, Post M. Similarities and dissimilarities of branching and septation during lung development. *Pediatr Pulmonol* 2005;40: 113–134.
24. Gerhardt H, Golding M, Fruttiger M, Ruhrberg C, Lundkvist A, Abramsson A, Jeltsch M, Mitchell C, Alitalo K, Shima D, *et al*. VEGF guides angiogenic sprouting utilizing endothelial tip cell filopodia. *J Cell Biol* 2003;161:1163–1177.
25. Kunig AM, Balasubramaniam V, Markham NE, Morgan D, Montgomery G, Grover TR, Abman SH. Recombinant human vegf treatment enhances alveolarization after hyperoxic lung injury in neonatal rats. *Am J Physiol Lung Cell Mol Physiol* 2005;289:L529–L535.
26. Gerety SS, Wang HU, Chen ZF, Anderson DJ. Symmetrical mutant phenotypes of the receptor EphB4 and its specific transmembrane ligand ephrin-B2 in cardiovascular development. *Mol Cell* 1999;4:403–414.
27. Wang HU, Chen ZF, Anderson DJ. Molecular distinction and angiogenic interaction between embryonic arteries and veins revealed by ephrin-B2 and its receptor Eph-B4. *Cell* 1998;93:741–753.
28. Favre CJ, Mancuso M, Maas K, McLean JW, Baluk P, McDonald DM. Expression of genes involved in vascular development and angiogenesis in endothelial cells of adult lung. *Am J Physiol Heart Circ Physiol* 2003;285:H1917–H1938.
29. Schwarz MA, Caldwell L, Cafasso D, Zheng H. Emerging pulmonary vasculature lacks fate specification. *Am J Physiol Lung Cell Mol Physiol* 2009;296:L71–L81.
30. Wilkinson GA, Schittny JC, Reinhardt DP, Klein R. Role for ephrinB2 in postnatal lung alveolar development and elastic matrix integrity. *Dev Dyn* 2008;237:2220–2234.
31. Nikolova Z, Djonov V, Zuercher G, Andres AC, Ziemiecki A. Cell-type specific and estrogen dependent expression of the receptor tyrosine kinase EphB4 and its ligand ephrin-B2 during mammary gland morphogenesis. *J Cell Sci* 1998;111:2741–2751.
32. Munarini N, Jager R, Abderhalden S, Zuercher G, Rohrbach V, Loercher S, Pfanner-Meyer B, Andres AC, Ziemiecki A. Altered mammary epithelial development, pattern formation and involution in transgenic mice expressing the EphB4 receptor tyrosine kinase. *J Cell Sci* 2002;115:25–37.
33. Hafner C, Meyer S, Hagen I, Becker B, Roesch A, Landthaler M, Vogt T. Ephrin-B reverse signaling induces expression of wound healing associated genes in IEC-6 intestinal epithelial cells. *World J Gastroenterol* 2005;11:4511–4518.
34. Maekawa H, Oike Y, Kanda S, Ito Y, Yamada Y, Kurihara H, Nagai R, Suda T. Ephrin-B2 induces migration of endothelial cells through the phosphatidylinositol-3 kinase pathway and promotes angiogenesis in adult vasculature. *Arterioscler Thromb Vasc Biol* 2003;23:2008–2014.
35. Steinle JJ, Meininger CJ, Forough R, Wu G, Wu MH, Granger HJ. Eph B4 receptor signaling mediates endothelial cell migration and proliferation via the phosphatidylinositol 3-kinase pathway. *J Biol Chem* 2002;277:43830–43835.
36. Soll RF, Morley CJ. Prophylactic versus selective use of surfactant in preventing morbidity and mortality in preterm infants. *Cochrane Database Syst Rev* 2001;2.
37. Katsu M, Koyama H, Maekawa H, Kurihara H, Uchida H, Hamada H. Ex vivo gene delivery of ephrin-B2 induces development of functional collateral vessels in a rabbit model of hind limb ischemia. *J Vasc Surg* 2009;49:192–198.
38. Mansson-Broberg A, Siddiqui AJ, Genander M, Grinnemo KH, Hao X, Andersson AB, Wardell E, Sylven C, Corbascio M. Modulation of ephrinB2 leads to increased angiogenesis in ischemic myocardium and endothelial cell proliferation. *Biochem Biophys Res Commun* 2008; 373:355–359.
39. Jankov RP, Kantores C, Belcastro R, Yi M, Tanswell AK. Endothelin-1 inhibits apoptosis of pulmonary arterial smooth muscle in the neonatal rat. *Pediatr Res* 2006;60:245–251.
40. Campbell AI, Zhao Y, Sandhu R, Stewart DJ. Cell-based gene transfer of vascular endothelial growth factor attenuates monocrotaline-induced pulmonary hypertension. *Circulation* 2001;104:2242–2248.
41. Sawamiphak S, Seidel S, Essmann CL, Wilkinson GA, Pitulescu ME, Acker T, Acker-Palmer A. Ephrin-B2 regulates VEGFR2 function in developmental and tumour angiogenesis. *Nature* 2010;465:487–491.
42. Wang Y, Nakayama M, Pitulescu ME, Schmidt TS, Bochenek ML, Sakakibara A, Adams S, Davy A, Deutsch U, Luthi U, *et al*. Ephrin-B2 controls VEGF-induced angiogenesis and lymphangiogenesis. *Nature* 2010;465:483–486.
43. Korff T, Braun J, Pfaff D, Augustin HG, Hecker M. Role of ephrinB2 expression in endothelial cells during arteriogenesis: impact on smooth muscle cell migration and monocyte recruitment. *Blood* 2008;112:73–81.

ON LINE SUPPLEMENT

Critical Role of the Axonal Guidance Cue EphrinB2 in Lung Growth, Angiogenesis and Repair

Arul Vadivel, PhD, Tim van Haaften, MSc, Rajesh S Alphonse, MBBS, MSc, Gloria-Juliana Rey-Parra, MD, Lavinia Ionescu, MD, Al Haromy, MSc, Farah Eaton, Evangelos Michelakis, MD, and Bernard Thébaud, MD, PhD, FRCPC

Methods

All procedures were approved by the Institutional Animal Care and Use Committee at the University of Alberta.

***In vivo* EphrinB2 knock down using small interfering RNA (siRNA).** Lung EphrinB2 was inhibited using intranasal EphrinB2 siRNA (Ambion, Austin, TX) administration (4μg/g in 2.5μl/g) (1) to rat pups at postnatal day (P) 4, P7, and P10. For this *in vivo* experiment, we opted for an intranasal approach as it allows repetitive and targeted administration at the desired time points during alveolar development to assess the role of EphrinB2 during this crucial period of lung development. This technique has been used effectively by us and other investigators for gene silencing in the lung (1-3). Lungs were harvested at P14 to assess EphrinB2 expression and lung morphometry.

Immunoblotting. Protein expression in whole lungs was measured with immunoblotting as previously described (4) using commercially available antibodies. The intensity of the bands was normalized to the intensity of a reporter protein (actin) using the Kodak Gel-doc system. EphB4 antibody was obtained from Santa Cruz Biotechnology Inc (Santa Cruz, CA) and Caspase 3 from Abcam (ab13847, Cambridge, MA, USA).

Lung endothelial cell isolation. Under strictly aseptic conditions, lungs were chopped using surgical blades and scissors into small pieces (approximately 1-2 mm^2). The pieces were suspended in collagenase/dispase digestive solution (0.1U collagenase and 0.8U dispase/mL) (Roche Applied Science, Laval, QC) at 37°C for 1 hour with intermittent shaking. A single cell suspension was obtained by straining the lung digest through 70 and 40 mm cell strainers. After washing in DMEM with 10% fetal calf serum, the cells were resuspended in phosphate buffered saline (PBS) containing 0.1% (w/v) bovine serum albumin (BSA) and incubated with streptavidin tagged dynabeads (Dynal, Invitrogen, Burlington, ON) pretreated with biotinylated anti-rat CD31 antibody (Abcam, Cambridge, MA). Dynabead tagged CD31 positive cells were selected out using a magnetic separator and made into a

pellet by centrufugation (300 g). The cell pellets were snap frozen in liquid nitrogen and stored in -80°C until use.

Lung morphometry. Lungs were fixed with a 10% formaldehyde solution through the trachea under at a constant pressure of 20 cmH_2O as previously described (4, 5). Alveolar structures were quantified on systematically sampled lung sections on a motorized microscope stage using the mean linear intercept (4, 5).

Barium-gelatin angiograms and arterial density counts. A barium-gelatin mixture (60ºC) was infused in the main pulmonary artery until surface filling of vessels with barium was seen uniformly over the surface of the lung as previously described (4, 5). Six animals/group, five sections/lung and ten high-power fields/section were counted.

Oxygen-induced lung injury. Rat pups were exposed to normoxia (21% O_2, control group) or hyperoxia (95% O_2, BPD-group) from birth to P14 in sealed Plexiglas chambers (BioSpherix, Redfield, NY) with continuous O_2 monitoring (4, 5). Dams were switched every 48 hours between the hyperoxic and normoxic chambers to prevent damage to their lungs and provide equal nutrition to each litter. Litter size was adjusted to 12 pups to control for effects of litter size on nutrition and growth. Rat pups were euthanized at P21 with intraperitoneal pentobarbital and lungs and heart were processed, according to the performed experiments.

Quantitative Real-Time Polymerase Chain Reaction. LCM specimens were analyzed by quantitative real-time polymerase chain reaction (qRT-PCR) using specific primers. Primers for each gene were designed by use of Primer Express software. Total RNA was extracted using an RNEasy Mini Kit (Qiagen, Mississauga, ON). The TaqMan One-Step RT-PCR Master Mix reagent kit (Applied Biosystems, Carlsbad, CA) was used to quantify the copy number of cDNA targets. Levels of mRNA were normalized to a housekeeping gene (18S rRNA) and expressed as $2^{\Delta\Delta Ct}$, as described previously (4, 5). TaqMan Gene expression assay kits (assay ID are in parentheses) for EphrinB2 (Rn01756899_m1), EphA4 (Rn02114236_s1), EphB2 (Rn01181017_m1), EphrinA1 (Rn00585955_m1), and EphrinB1 (Rn00438666_m1)

were purchased from Applied Biosystems.

Immunofluorescence using confocal microscopy. Immunofluorescence was performed on paraffin embedded sections as previously described (4, 5).

Isolation and O_2-exposure of alveolar epithelial type 2 cells (AEC2). AEC2 were isolated from time-dated fetal day 19.5 rat lungs as previously described, using serial differential adhesions to plastic and low-speed centrifugations (5, 6).

***In Vitro* AEC2 Cell Viability Assay**. After 48 hrs of culture in normoxic (control) or hyperoxic conditions, cell viability was evaluated by measuring the mitochondrial-dependent reduction of colorless 3-(4,5-Dimethylthiazol-2-yl)- 2,5- diphenyltetrazolium bromide (MTT) (Invitrogen, Eugene, Oregon, USA) to blue colored formazan which was dissolved in dimethyl sulfoxide and the absorbance of each sample was spectrophotometrically measured at 550 nm with a Spectra Max 190 (Molecular Devices) microplate reader.

Cell cycle analysis by DNA Content. Rat lung microvascular endothelial cells (RLMVEC) were plated in 25 cm^2 tissue culture flasks and cultured in MCDB-131 Complete medium (VEC Technologies, INC., Rensselaer, NY) either in normoxic or hyperoxic (95% oxygen) with or without EphrinB2 supplementation [0.5µg/ml]. After 48 hrs of culture, the cells were fixed in cold 100% ethanol and stored at -20^{o}C until use. For cell cycle analysis, cells were stained with propidium iodide solution (Sigma) in the presence of 0.1% Triton X and 0.02% DNase free RNase A (Sigma). Nonclumped cells were gated out and displayed with DNA area (linear red fluorescence) on x-axis versus cell number on the y-axis for cell-cycle analysis using Cellquest (Beckton Dickinson) and FlowJo (version 5.7.2) software.

Wound Healing Assay with Fetal Rat AEC2. AEC2 (10^6 cells/ml) were seeded into a plastic 24-well cell culture plate. At about 36 hours, the cell monolayer was scraped with a p200 pipette tip and medium was replaced with DMEM or DMEM supplemented with EphrinB2 [0.5µg/ml]. The surface area of the wound was recorded over time with OpenLab (Quorum Technologies Inc, Guelph, ON, Canada) (5).

Isolation and proliferation of pulmonary microvascular endothelial cells (PMVEC). PMVEC were isolated from room air and hyperoxia exposed newborn rat lungs, as described by King et al (14). Briefly, the outer edges of the lungs were carefully dissected and placed in a 60-mm dish containing cold DMEM (4°C). Tissue was digested with type II collagenase (Worthington), rinsed with DMEM and cultured in DMEM enriched with 20% FBS (Hyclone) and 100 U/ml penicillin-100 μg/ml streptomycin (GIBCO) at 37°C with 5% CO_2-21% O_2 and passages 3-5 were used for consecutive experiments. PMVEC from the four different treatment groups were seeded in 48-well cell culture plates at a density of 10^4 cells/well and allowed to attach over 24 hrs. Following medium change on day-2 the cells were allowed to grow for 9 days and their viability was evaluated at 72hr intervals using the MTT assay.

Endothelial network formation assay. The formation of cord-like structures by PMVEC was assessed in Matrigel coated wells. PMVEC from normal newborn rat lungs (40,000 cells/well) were seeded into 48-well plates coated with Matrigel (BD Biosciences, Mississauga, ON) into groups of triplicates: (1) Normoxia (21% O_2), (2) Normoxia+EphrinB2 (0.5μg/ml), (3) Hyperoxia (95% O_2), (4) Hyperoxia+EphrinB2 (0.5μg/ml) and incubated at 37°C for 8–12h. Cord-like structures were observed using an inverted phase contrast microscope (Leica, Richmond Hill, ON, Canada) and quantified by measuring the number of intersects and the length of structures in random fields from each well using OpenLab (Quorum Technologies Inc, ON, Canada).

***In vivo* EphrinB2 treatment.** Newborn rat pups were allocated to 4 groups: 1) normoxia (21%, control group), 2) normoxia+Ephrin B2, 3) hyperoxia (95% O_2, BPD-group), and 4) hyperoxia+Ephrin B2. Ephrin B2/Fc (R&D Systems, Inc. Minneapolis, MN, USA, 2μg/200g/day diluted in sterile distilled water) (15) was administered intranasally daily from P4 to P14.

EphrinB2 ELISA. Tissue was weighed and homogenized at 50 mg tissue per mL of

1X PBS + 0.05% TWEEN-20 (Sigma Cat# P5927) and 0.1uL/mL Protease inhibitor cocktail (sigma Cat# P8340). Tissue suspension was centrifuged at 10000xg for 10 min at 4 degrees C and supernatant was collected and stored at -80 until assay. Lung homogenates were assayed for EphrinB2 using an ELISA Kit for Ephrin B2 (EFNB2) from USCNLife (Wuhan, China). Results are expressed as ng/mL.

Scanning electron microscopy (SEM) of alveolar structures. SEM was performed as previously described (3, 4).

Echo-doppler. Pulmonary artery acceleration time, expressed as a ratio over the right ventricular ejection time (PAAT/RVET), was assessed by Doppler echocardiography as previously described (5, 7).

Right ventricular hypertrophy (RVH) and pulmonary artery remodeling. Right ventricle and left ventricle plus septum were weighed separately to determine the right ventricle to left ventricle+septum ratio (RV/LV+S) as an index of RVH (8). To assess pulmonary artery remodeling, the medial wall thickness (MWT) was calculated as (external diameter-lumen diameter)/vessel diameter (8).

Statistics. Values are expressed as the mean±SEM. Statistical comparisons were made with the use of ANOVA. Post hoc analysis used a Fisher's probable least significant difference test (Statview 5.1, Abacus Concepts, Berkeley, CA). A value of $P<0.05$ was considered statistically significant.

References

1. Bitko V, Musiyenko A, Shulyayeva O, Barik S. Inhibition of respiratory viruses by nasally administered sirna. *Nat Med* 2005;11:50-55.

2. Massaro D, Massaro GD, Clerch LB. Noninvasive delivery of small inhibitory rna and other reagents to pulmonary alveoli in mice. *Am J Physiol Lung Cell Mol Physiol* 2004;287:L1066-1070.

3. Vadivel A, Abozaid S, van Haaften T, Sawicka M, Eaton F, Chen M, Thebaud B. Adrenomedullin promotes lung angiogenesis, alveolar development, and repair. *Am J Respir Cell Mol Biol* 2010;43:152-160.

4. Thebaud B, Ladha F, Michelakis ED, Sawicka M, Thurston G, Eaton F, Hashimoto K, Harry G, Haromy A, Korbutt G, Archer SL. Vascular endothelial growth factor gene therapy increases survival, promotes lung angiogenesis, and prevents alveolar damage in hyperoxia-induced lung injury: Evidence that angiogenesis participates in alveolarization. *Circulation* 2005;112:2477-2486.

5. van Haaften T, Byrne R, Bonnet S, Rochefort GY, Akabutu J, Bouchentouf M, Rey-Parra GJ, Galipeau J, Haromy A, Eaton F, Chen M, Hashimoto K, Abley D, Korbutt G, Archer SL, Thebaud B. Airway delivery of mesenchymal stem cells prevents arrested alveolar growth in neonatal lung injury in rats. *Am J Respir Crit Care Med* 2009;180:1131-1142.

6. Alphonse RS, Vadivel A, Coltan L, Eaton F, Barr AJ, Dyck JR, Thebaud B. Activation of akt protects alveoli from neonatal oxygen-induced lung injury. *Am J Respir Cell Mol Biol* 2011;44:146-154.

7. Bonnet S, Michelakis ED, Porter CJ, Andrade-Navarro MA, Thebaud B, Bonnet S, Haromy A, Harry G, Moudgil R, McMurtry MS, Weir EK, Archer SL. An abnormal mitochondrial-hypoxia inducible factor-1alpha-kv channel pathway disrupts oxygen sensing

and triggers pulmonary arterial hypertension in fawn hooded rats: Similarities to human pulmonary arterial hypertension. *Circulation* 2006;113:2630-2641.

8. Ladha F, Bonnet S, Eaton F, Hashimoto K, Korbutt G, Thebaud B. Sildenafil improves alveolar growth and pulmonary hypertension in hyperoxia-induced lung injury. *Am J Respir Crit Care Med* 2005;172:750-756.